UCID- 17516

Lawrence Livermore Laboratory

STABLE PROPAGATION OF A HIGH-CURRENT ELECTRON BEAM:
EXPERIMENTAL OBSERVATIONS AND COMPUTATIONAL MODELING

R. Briggs, J. Clark, T. Fessenden, E. Lee, and E. Lauer

August 1, 1977

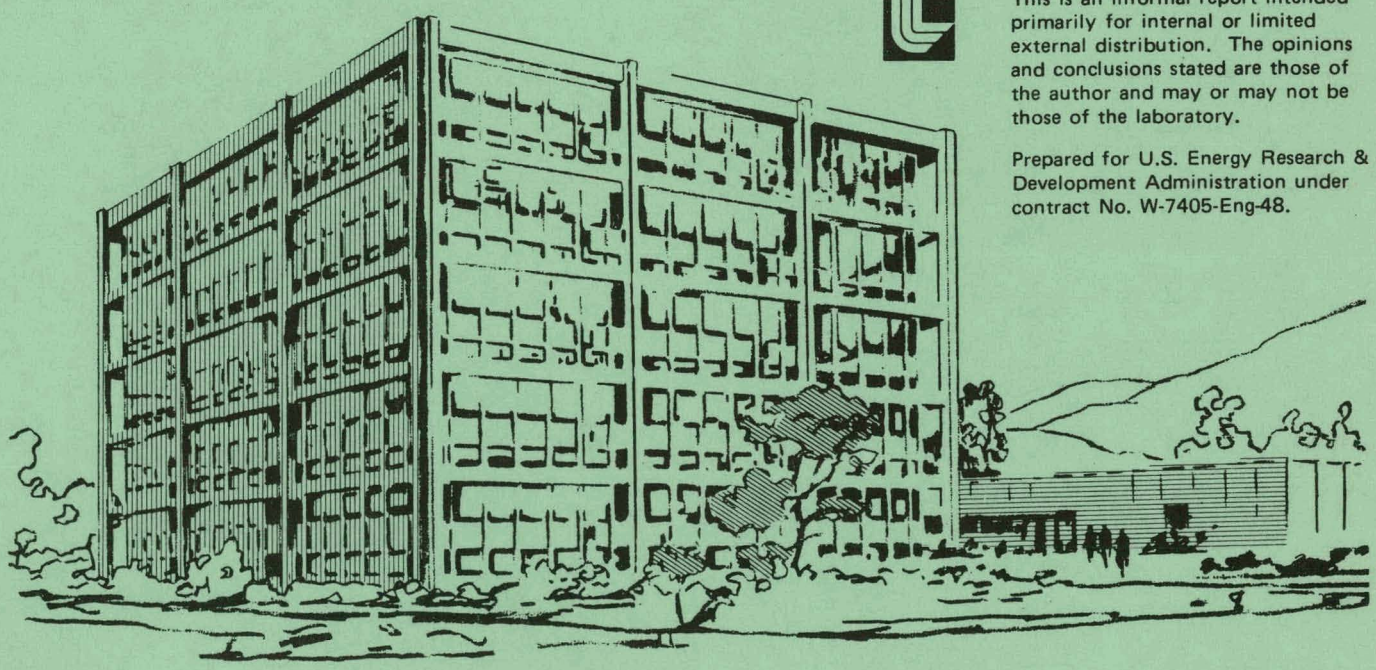

Prepared for U.S. Energy Research & Development Administration under contract No. W-7405-Eng-48.

DISCLAIMER

THIS PAGE

WAS INTENTIONALLY

LEFT BLANK

CONTENTS

STABLE PROPAGATION OF A HIGH-CURRENT ELECTRON BEAM: EXPERIMENTAL OBSERVATIONS AND COMPUTATIONAL MODELING

ABSTRACT

Experimental studies of self-focused, high-current electron-beam propagation phenomena are compared with the results of computational modeling. The model includes the radial structure of the beam-plasma system, a full electromagnetic field description, primary and secondary gas ionization processes, and a linear theory of the hose-like distortions. Good agreement between the experimental results and the computations strengthens the premise that hose instability is the principal limitation to propagation at high pressure.

INTRODUCTION

Hose instability severely limits the propagation of self-focused electron beams in neutral gases, as has been amply demonstrated in the Astrom beam experiments. The observation of stable propagation with a high-current, 1.5-MeV, diode-produced beam[1,2] is, therefore, quite significant, since it demonstrates that stability against hose distortions can be achieved under the proper conditions.

Recently, a computional model of beam propagation and linear hose instability has been developed. This model successfully describes the behavior of our pulsed-diode electron beam at pressures above 1 Torr. Thus, this report presents (1) some of the most recent experimental observations, (2) a description of the above computational model (EMPULSE code), and (3) a comparison of experimental and code results.

EXPERIMENTAL OBSERVATIONS

The electron beam used in these experiments was generated by an FX-25 device manufactured by Ion Physics Corporation. The beam current has a rise time of approximately 4 ns to 7.5 kA, and then a slower rise reaching 15 kA at 15 ns. The beam contains about 500 J at a peak voltage of 1.5 MeV. The experimental apparatus is shown in Fig. 1. The electron beam passes through

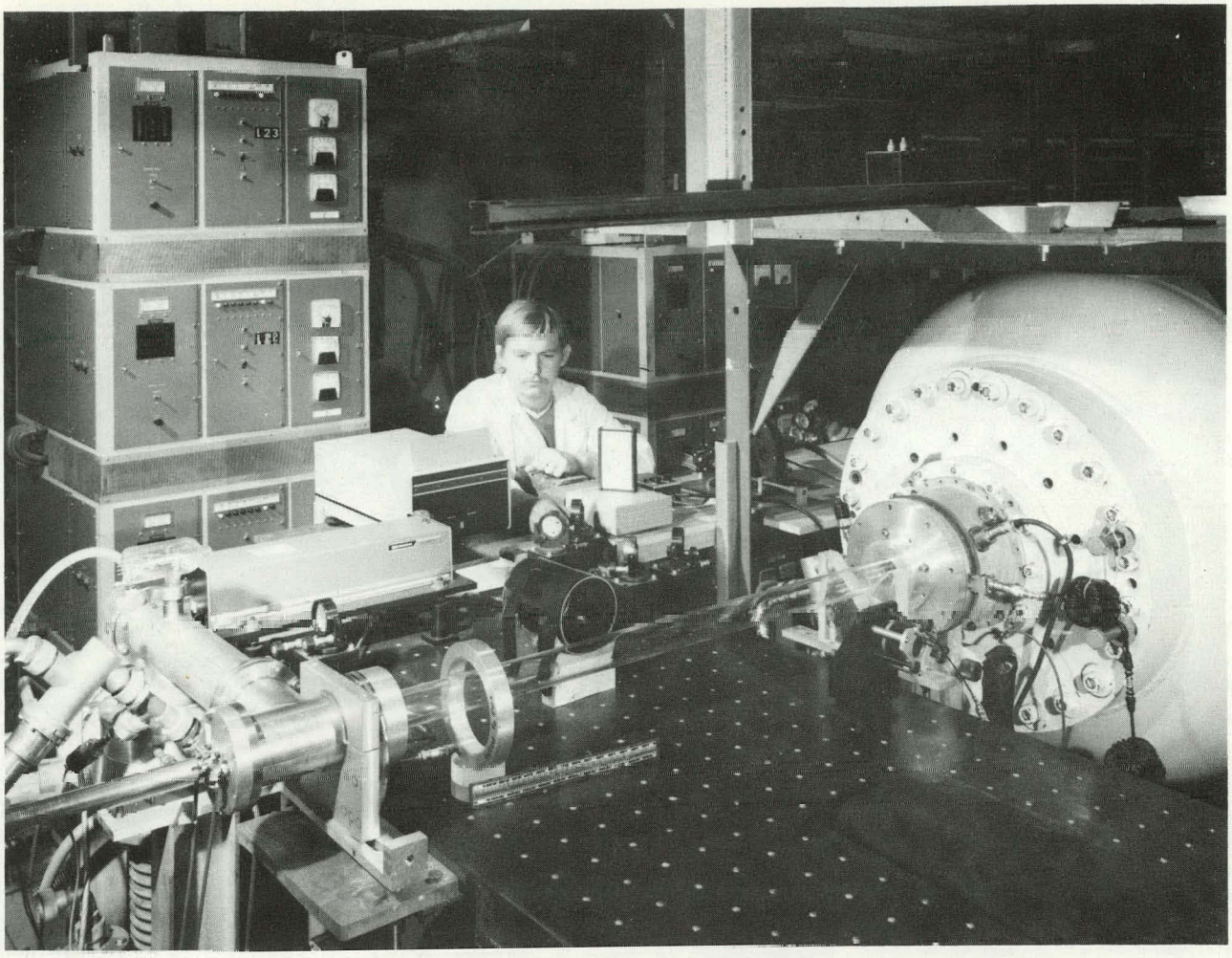

Fig. 1. Experimental apparatus showing Lucite drift tube.

a 0.0025-cm (1-mil) titanium anode into a Lucite drift tube and is collected by the 4.8-cm Faraday cup/calorimeter described in previous reports.[1,2] A 0.0025-cm aluminized Mylar foil placed over the Faraday cup/calorimeter excludes the plasma current and acts as a witness plate. The distance between the anode and the Faraday cup/calorimeter was adusted to control the beam propagation length.

Figure 2 shows open-shutter photographs of the electron beam propagating in neon inside a 180-cm, 25-cm i.d. Lucite tube. For the upper photographs, the tube was lined with a copper screen that connected the Faraday cup to the FX-25 and terminated the electromagnetic fields generated by the beam inside the tube. For the lower photographs, the tube was not lined with a copper screen. In neon, the beam propagates very stably at 5 Torr, while hose instability can be seen even with open-shutter photography at the higher pressures ($\approx$50 Torr). Note that the presence or absence of the copper screen liner has little effect on beam propagation at the pressures shown.

Figure 3 shows the energy propagated by the beam through a 120-cm long, 8.8-cm i.d. tube as a function of pressure for various gases. Here the presence of a propagation window at a few Torr is clearly demonstrated; the pressure range of the propagation window depends on the gas.

Figure 4 shows oscillograms of the beam current delivered to the Faraday cup/calorimeter at a propagation distance of 100 cm at pressures from 0.05 to 20 Torr air. The data was taken with a 120-cm long, 8.8-cm. i.d. tube with a copper screen lining. At the lowest pressure, the beam does not propagate until the gas is sufficiently ionized to short out the radial electric field, thereby allowing the beam to self-focus. As the pressure is increased, the beam self-focuses earlier in the pulse, with an increase in the total energy transmitted. These phenomena are characteristic of the "low pressure window" mode of propagation first identified in experiments with the Astron beam. At 0.2 Torr the time of space charge neutralization occurs approximately halfway through the pulse. At this pressure, the peak current measured by the Faraday cup/calorimeter is greater than the current generated by the FX-25. This is the "current amplification" phenomenom also seen in the Astron experiments. At pressures up to 5 Torr, the beam propagates well, with nearly all the energy transmitted to the Faraday cup/calorimeter. At 10 Torr, the tail of the pulse is strongly eroded, and only about 40% of the beam energy is collected by the Faraday cup/calorimeter. At 20 Torr, the degree of tail erosion is even greater. Other experiments have shown that at pressures of 10 or

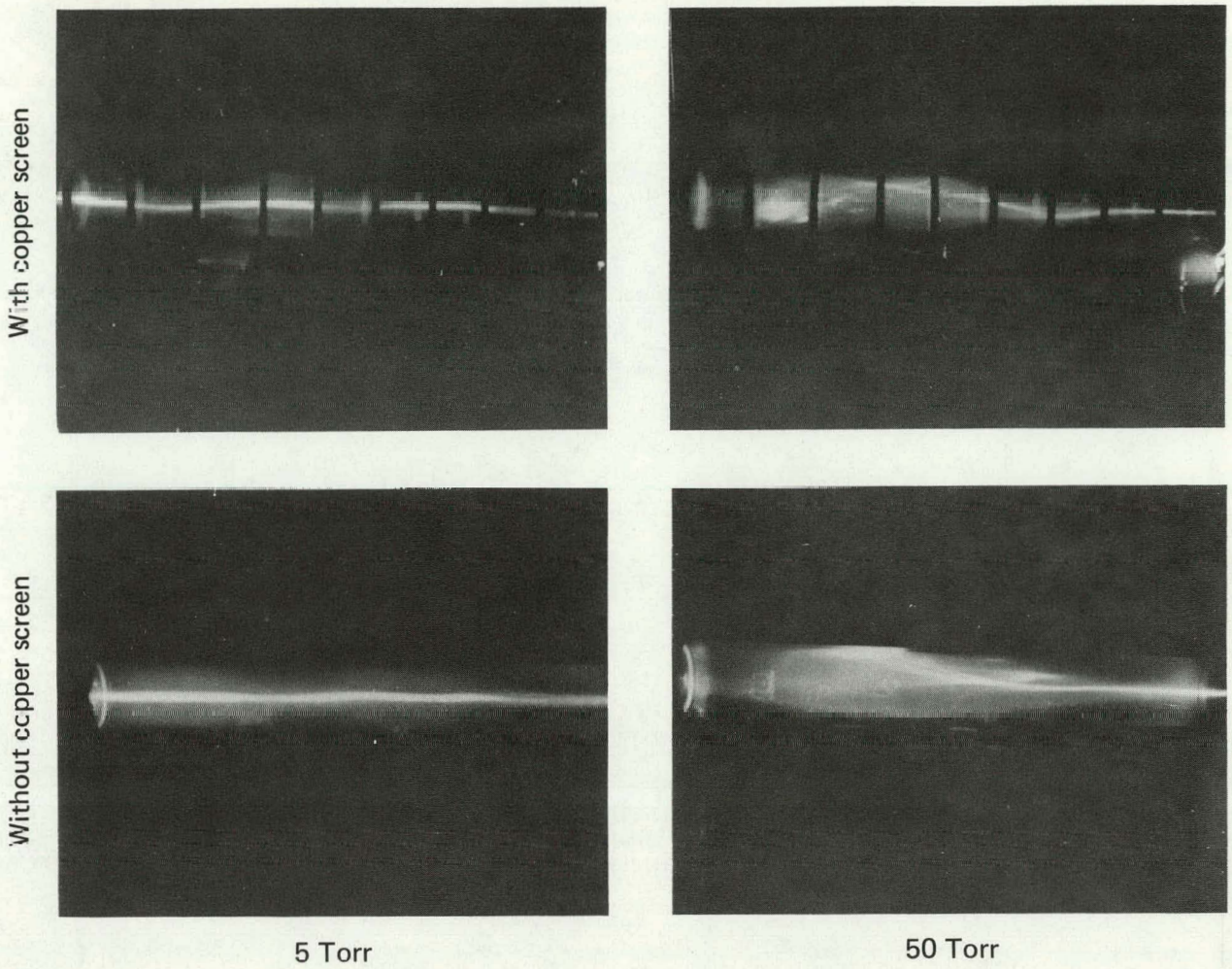

Fig. 2. Open-shutter photographs of electron beam propagating inside a 180-cm long, 25-cm i.d. Lucite tube, with copper screen (upper) and without copper screen (lower), at neon gas pressures of 5 Torr (left) and 50 Torr (right).

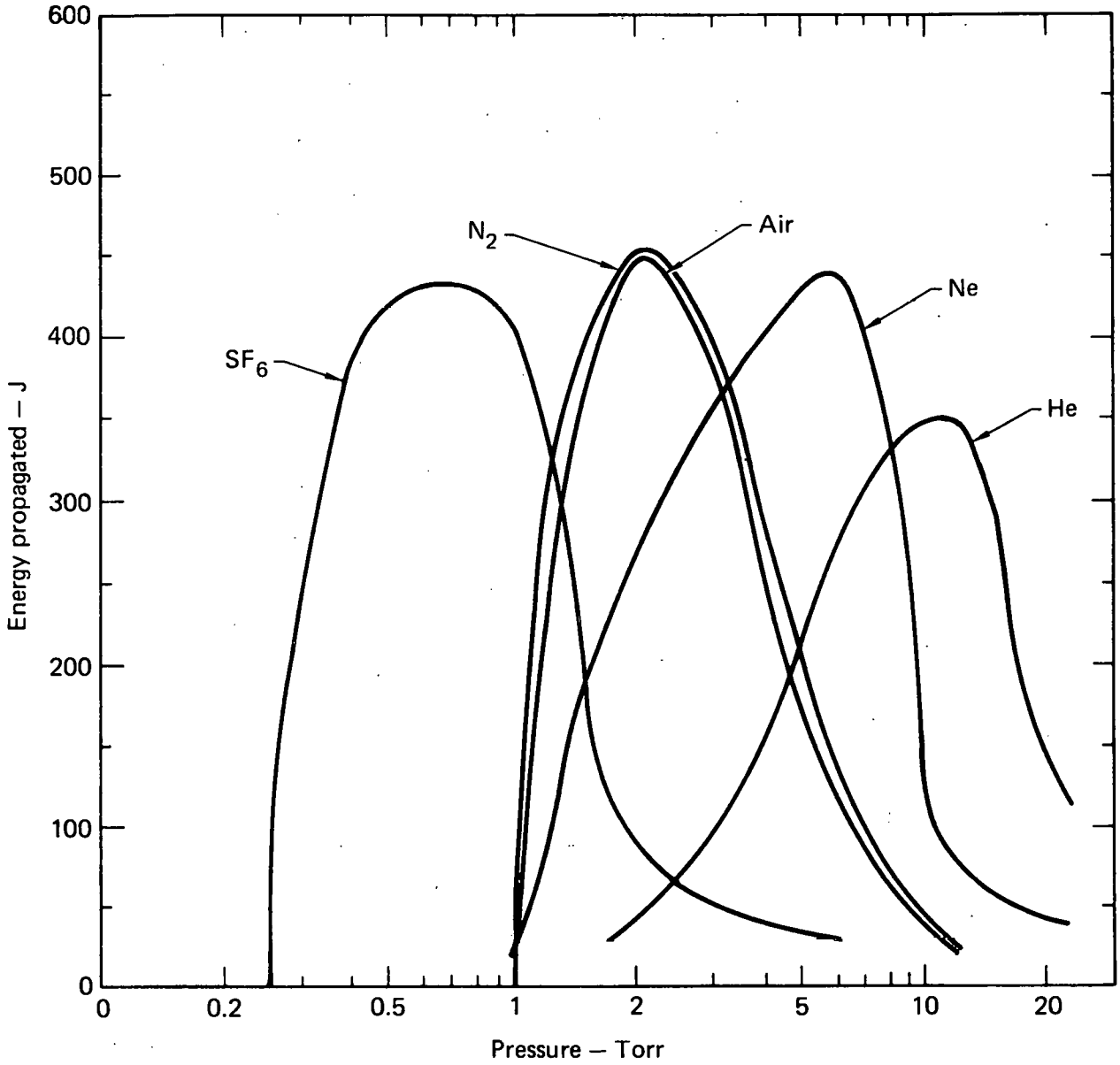

Fig. 3. Energy propagation window for various gases as a function of pressure, for 120-cm long, 8.8-cm i.d. tube, without copper screen.

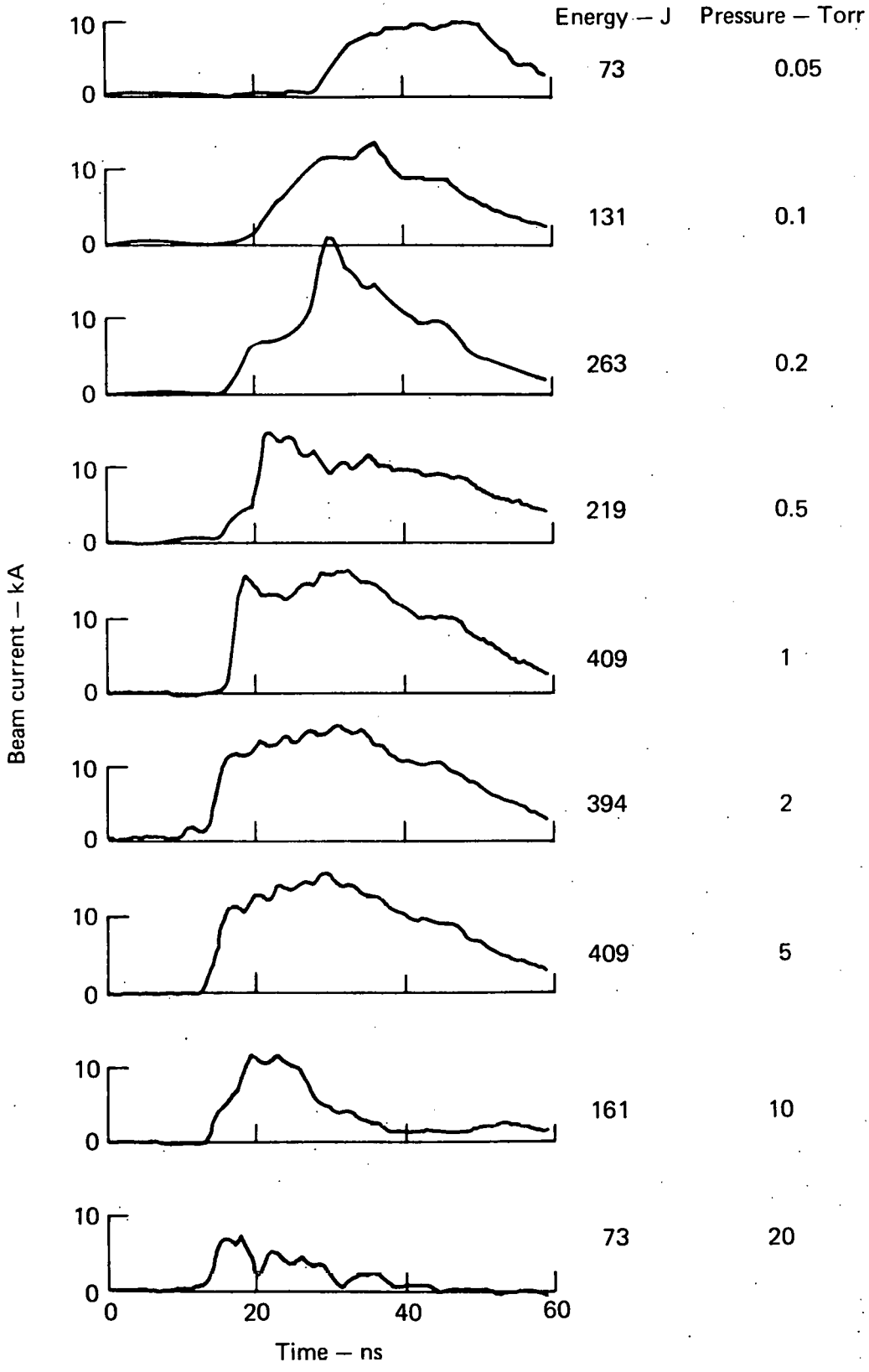

Fig. 4. Beam current delivered to Faraday cup/calorimeter at propagation distance of 100 cm and at air pressures of from 0.05 to 20 Torr, for 120-cm long, 8.8-cm i.d. tube, with copper screen.

20 Torr the tail erosion also increases rapidly with propagation length.

Figure 5 shows an open-shutter photograph of the beam propagating in air at 2 Torr in a 550-cm long, 8.8-cm i.d. tube. (The length of the tube was limited only by the space available in the experimental area.) Here, the beam energy delivered to the Faraday cup/calorimeter exceeded 250 J. Moreover, the beam was well focused at the collection point, as evidenced by a hole in the witness foil. The beam current oscillogram was very similar to those obtained at shorter propagation length, indicating that the energy loss has resulted from a loss of the average electron energy and not from a loss of beam electrons. At this pressure, the energy loss is primarily due to the collective electric field (ohmic loss) and not to the direct impact with gas molecules. The axial electric field predicted by the EMPULSE code (described in the following section) ranges from approximately 6 kV/cm near the pulse head ($\approx$0.5 ns point) to approximately 0.2 kV/cm in the body of the pulse. If we average this electric field over the pulse, an energy loss of 200 to 300 keV per particle over the 550-cm distance is predicted, which is in reasonable agreement with the experimental observation, considering the uncertainty in the mean particle energy at the anode.

In summary, the data show that in air at a pressure of 2 Torr the beam propagates with no evidence of instability. At higher pressures, the beam is lost by an erosion that proceeds from the tail of the beam toward the head when either pressure or propagation length is increased. At lower pressures, the beam is not well guided by an unscreened Lucite tube. The addition of a conducting wall inside the tube improves the propagation at lower pressures and we see evidence of the "low pressure window" and "current amplification" phenomena previously observed in experiments with the Astron beam.

COMPUTATIONAL STUDY

The beam-propagation code, EMPULSE, has been used to simlate the FX-25 experiments performed in low pressure air. The main purpose of this study is to determine whether the code model is consistent with the observations of suppressed hose growth at the lower gas pressures (1 to 5 Torr), and the disruption seen at higher pressures. A simple analytical model of hose growth[3] has indicated the important role played by the avalanching of conductivity by electric field breakdown, but detailed modeling of this phenomenon can only be made with EMPULSE.

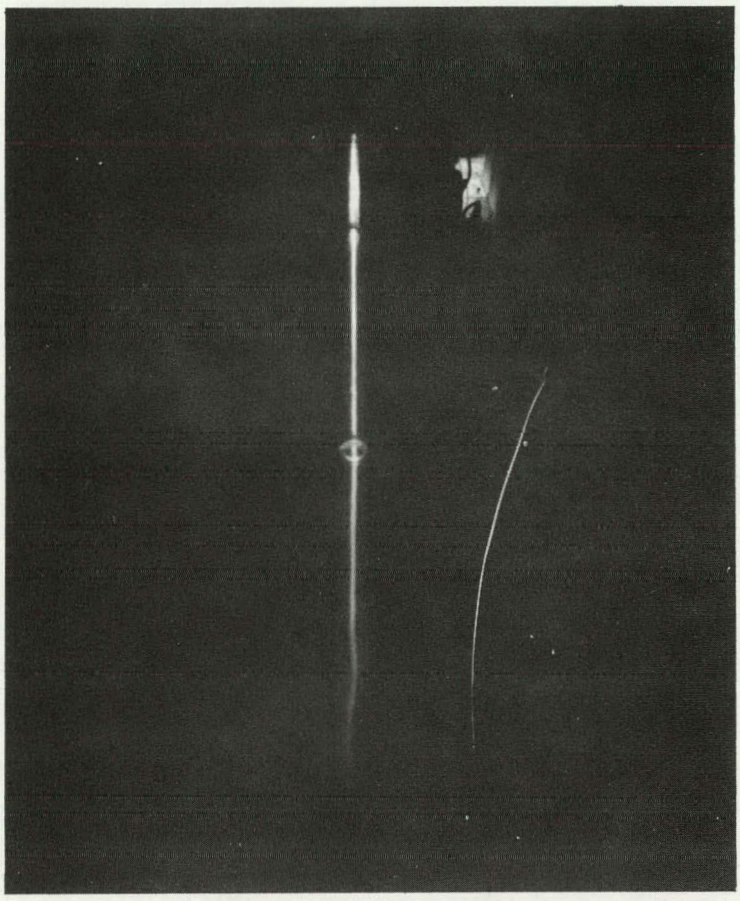

Fig. 5. Open-shutter photograph of beam propagating at an air pressure of 2 Torr inside a 550-cm long, 8.8-cm i.d. tube, without copper screen.

Clearly, this experimental study provides an important test case for the code; a successful simulation of the data would give a higher degree of confidence in the predictions it makes in other regimes.

It must be emphasized that the experiments at pressures below 1 Torr are not properly simulated by EMPULSE. The code cannot treat microinstabilities (e.g., the two-stream mode), while there is considerable evidence that propagation is actually limited by such phenomena at pressures of about 1 Torr and below. The code is designed to treat the higher pressure regime in which resistive effects, such as the hose instability, are expected to play the dominant role.

Description of EMPULSE

EMPULSE numerically models a highly relativistic, self-focused, electron beam propagating in a gas without externally applied fields. The current is assumed low compared with the Alfvén limit, so the paraxial approximation is adopted for the beam dynamics. The principal features are as follows:

(1) The electromagnetic field is treated with two components of potential (A_z and ϕ), where Maxwell's equations are solved taking the beam velocity equal to the speed of light. A full discussion of these field equations is given in another report.[4]

(2) The plasma channel is characterized by scalar electrical conductivity, generated by the passage of the beam through the gas. The conductivity is given by

$$\sigma = \frac{n_e e^2}{m\nu_m},$$

where ν_m is the momentum transfer frequency between plasma electrons and gas molecules, and n_e is the plasma electron density. For the set of runs described below we take

$$\nu_m = 1.8 \times 10^{-7}\, n_g \ (s^{-1}),$$

where n_g is the number density of the gas. This value is a good approximation if electron temperature is in the expected range 1 to 10 eV.

The electron density, n_e, is generated by direct ionization of the gas by the beam and by avalanching in the induced electric field; i.e.,

$$\frac{\partial n_e}{\partial t} = \kappa\, n_g \frac{J_b}{e} + \nu^i n_e \quad .$$

Here, J_b is beam current density, and $\kappa = 2.36 \times 10^{-18}\ \mathrm{cm}^2$ is the effective ionization cross section for 1.5 MeV electrons (the cascade factor is taken into account). The avalanche rate ν^i is a function of $|\underline{E}|/P$ fitted to the pulse breakdown data of Felsenthal and Proud.[5] We neglect recombination; this approximation is valid for all pressures except the highest ones ($\approx$100 Torr). For the undisturbed current density profile, the truncated Bennett form is used:

$$J_{b0}(r, x) = N(a)\, \frac{I_b(x)}{\pi a^2} \left(1 + \frac{r^2}{a^2}\right)^{-2} \left(1 - \frac{r^2}{R^2}\right)^2 \quad ,$$

with radial coordinate r, scale radius a(x), and channel radius R. Note that a, I_b, and normalizing factor N(a) are functions of the Doppler-shifted time variable,

$$x = ct - z \quad ,$$

but are not functions of z; i.e., the current profile is a fixed wave form. The particlular form used here is

$$I_b = I_0 \tanh\left(\frac{x}{L_r}\right) \tanh\left(\frac{L_p - x}{L_r}\right) \quad ,$$

with I_0 the peak current, L_r the rise length, and L_p the pulse length. The radius a is determined from the emittance ε (assumed constant) by the usual pinch condition

$$\frac{\varepsilon^2}{a^2} = \frac{e}{\gamma mc^2}\left(\overline{rB_\theta} - \overline{rE_r}\right) \quad ,$$

with the averages taken over the beam current profile. Since E_r and B_θ cancel at the beam front, it is necessary to impose a maximum radius; we somewhat arbitrarily take $a \leq 10$ cm.

(3) To treat hose instability, the four functions A_z, ϕ, σ, and J_b are each decomposed into two azimuthal components:

$$A_z = A_{z0} + A_{z1} \sin\theta ,$$

$$\phi = \phi_0 + \phi_1 \sin\theta ,$$

$$\sigma = \phi_0 + \sigma_1 \sin\theta ,$$

$$J_b = J_{b0} - \frac{\partial J_{b0}}{\partial r} Y \sin\theta .$$

The dipole components (those with sin θ dependence) are considered to be of small amplitude, so that linear analysis applies, but they vary rapidly in x and z as a manifestation of hose instability. The particular form for J_b is the rigid beam expression,[3,6] which corresponds to a simple sideways displacement of magnitude Y(z, x).

(4) The beam is composed of 300 to 500 segments of varying thickness, Δx, which do not intermix as the beam propagates in the +z direction. Each segment is itself composed of 100 disks with distributed relativistic mass to simulate the phase mixing effects of particle orbits due to the anharmonic pinch field. Each disk is thus propagated in z and characterized by displacement $Y_i(z, x)$ with i = 1,..., 100. The displacement of a segment as a whole is a distributed mean,

$$\overline{Y} = \sum_{i=1}^{100} Y_i f_i ,$$

with the f_i selected to be in accord with known properties of the Bennett profile.[3,6]

(5) The field equations are solved by standard finite difference methods. All sensitive calculations are second order accurate. Boundary conditions must be imposed at R; for the case at hand, we consider that the confining drift tube is a perfect conductor, so $A_{z0}(R) + A_{z1}(R) = 0$.

A typical run of the type reported here requires about 30 min computing time on the CDC 7600.

Parameters of Simulation

Five runs of EMPULSE were made to simulate propagation in the FX-25 diode experiments at pressures of 2, 5, 10, 20, 200 Torr air. The drift channel was bounded by a metal wall at R = 4.98 cm, and the parameters used for the model current waveform were

$$I_0 = 10 \text{ kA} , \quad L_r = 120 \text{ cm} , \quad L_p = 1200 \text{ cm} .$$

The beam energy was chosen to correspond to a peak voltage of 1.5 MeV ($\gamma = 4$). Emittance was selected such that the fully-pinched radius is a = 1 cm (with full charge neutralization and peak current I_0). As mentioned, the pulse head is expanded, with maximum radius of 10 cm. Hence, the actual profile of the head is determined by the truncation factor $(1 - r^2/R^2)^2$.

At the point of injection (z = 0), a perturbation of the form

$$Y(z = 0, x) = \cos\left(\frac{\pi x}{L_p}\right)$$

was applied. The entire pulse propagated to z_{max} = 400 cm (corresponding to about 15 betatron wavelengths for the fully pinched beam; the actual betatron wavelength is increased by a factor of 1 to 3 because of current neutralization). Fields, conductivity, beam radius, and beam displacement were determined as functions of x and z.

Results of Code Runs

Table 1 gives the most significant computed quantities for the described EMPULSE runs. "Net current," "electrical conductivity" on axis, plasma "electron density" on axis, and "beam radius" are given for the representative point x = 500 cm (roughly the middle of the pulse). These are equilibrium quantities and, as such, are independent of z. The "pinch point" is the position in the beam head at which self-focus effects create the pinch equilibrium. This is somewhat of an artifice of the manner in which the profile is handled, but it is considered a reasonable indicator of the "true beginning" of equilibrium. "Maximum displacement" gives the largest displacement Y(z, x) computed near the pulse midpoint at x ≈ 600 cm. Since the perturbed equations are linear, Y_{max} should be compared with the initial perturbation amplitude of unity. The "x point where hose amplification begins" gives the point in

Table 1. Computed behavior of beam-plasma system at several pressures. Net current, conductivity, electron density and beam radius are given for the point x = 500 cm. Conductivity and density are on-axis values. Maximum displacement is given for x = 600-cm point.

Gas pressure, Torr	Net current,[a] A	Electrical conductivity,[a] sec^{-1}	Electron density,[a] cm^{-3}	Beam radius,[a] cm	Pinch point, cm	Maximum displacement near x = 600 cm, cm	x point where hose amplification begins, cm
2	3960	4.9×10^{12}	2.5×10^{14}	2.01	9.4	1.0	–
5	4980	3.2×10^{12}	4.1×10^{14}	1.66	8.6	1.7	400
10	6250	2.3×10^{12}	5.9×10^{14}	1.39	8.9	3.5	225
20	7790	3.0×10^{12}	8.0×10^{14}	1.17	9.7	4.5	175
200	9600	9.8×10^{11}	5.0×10^{15}	1.02	12.4	200+	55

[a]Given for the point x = 500 cm.

the pulse where the oscillations begin to exceed the initial perturbation. Previous to this point, Y shows only damped oscillating behavior.

In Table 2, the dipole decay length for the point x = 500 cm is given. Its mean derivative with x is also estimated:

$$\lambda \equiv \frac{\pi\sigma a^2}{2c} \quad , \qquad \frac{d\lambda}{dx} \approx \frac{\lambda}{x} \quad .$$

These quantities are useful in the interpretation of computed hose growth. For comparison we note that, with direct ionization alone ($\nu_i = 0$), the conductivity rise is such that

$$(d\lambda/dx)_{direct} \approx 0.1 \quad .$$

Discussion of Results and Comparisons with the Experiments

We note first that the input for the five computations differ only in gas pressure. Further, the laws governing the generation of conductivity are such that if direct ionization were the only process producing n_e, then all the runs would be identical. The considerable differences among the runs can,

Table 2. Dipole decay length vs pressure. Here $\lambda \equiv \pi\sigma a^2/2c$ and $d\lambda/dx = \lambda/500$ cm is a rough mean through the pulse.

Pressure, Torr	2	5	10	20	200
λ, cm	1036	461	233	215	53.4
$d\lambda/dx$	2.07	0.923	0.465	0.430	0.106

therefore, be ascribed to the degree of ionization due to avalanching in the induced electric fields. The avalanching process is found to dominate conductivity formation at P = 2 Torr and is negligible at 200 Torr.

The ionization calculated by EMPULSE is in good agreement with the experimental measurements. In Fig. 6 the computed results from Table 1 are plotted along with experimental results (from Ref. 2.) for pressures up to 20 Torr (at 200 Torr, recombination will begin to limit the density, and this is not included in the version of the code used here). The agreement is better than might be expected at 1 Torr and above, considering the fact that the current waveform, the radial profile of the head, etc., is only an approximate representation of the experiment. We interpret the rapid increase of electron density seen in experiments below 2 Torr as the onset of two-stream instability, as mentioned under Experimental Observations.

The general pattern of the predictions for hose amplification is also in agreement with the experimental observations. To illustrate this, we present in Fig. 7 the experimentally determined beam pulse energy on a target (at 100 cm) vs pressure, overlaid with EMPULSE code prediction of the amplification factor (Y_{max}/Y_0), 600 cm into pulse. The presence of a stable "window" around 2 Torr can be seen to be in good agreement with the code prediction.

Some additional comments on the code results follow:

(1) In all runs, ionization is due primarily to the direct process for the first 10 cm of pulse. Hence, the pinch point is similar for all.

(2) In all runs, net current is close to beam current through the first 30 cm of pulse; thereafter, in the low pressure runs, the avalanching of σ tends to freeze in net current, causing I to fall well below I_b in the body of the pulse. But for high pressure, $I \approx I_b$ throughout the pulse.

(3) Beam radius should be given approximately by

$$Ia^2 \approx \text{constant}.$$

This is qualitatively born out. The deviations from this rule reflect the fact that the plasma and beam current density profiles differ.

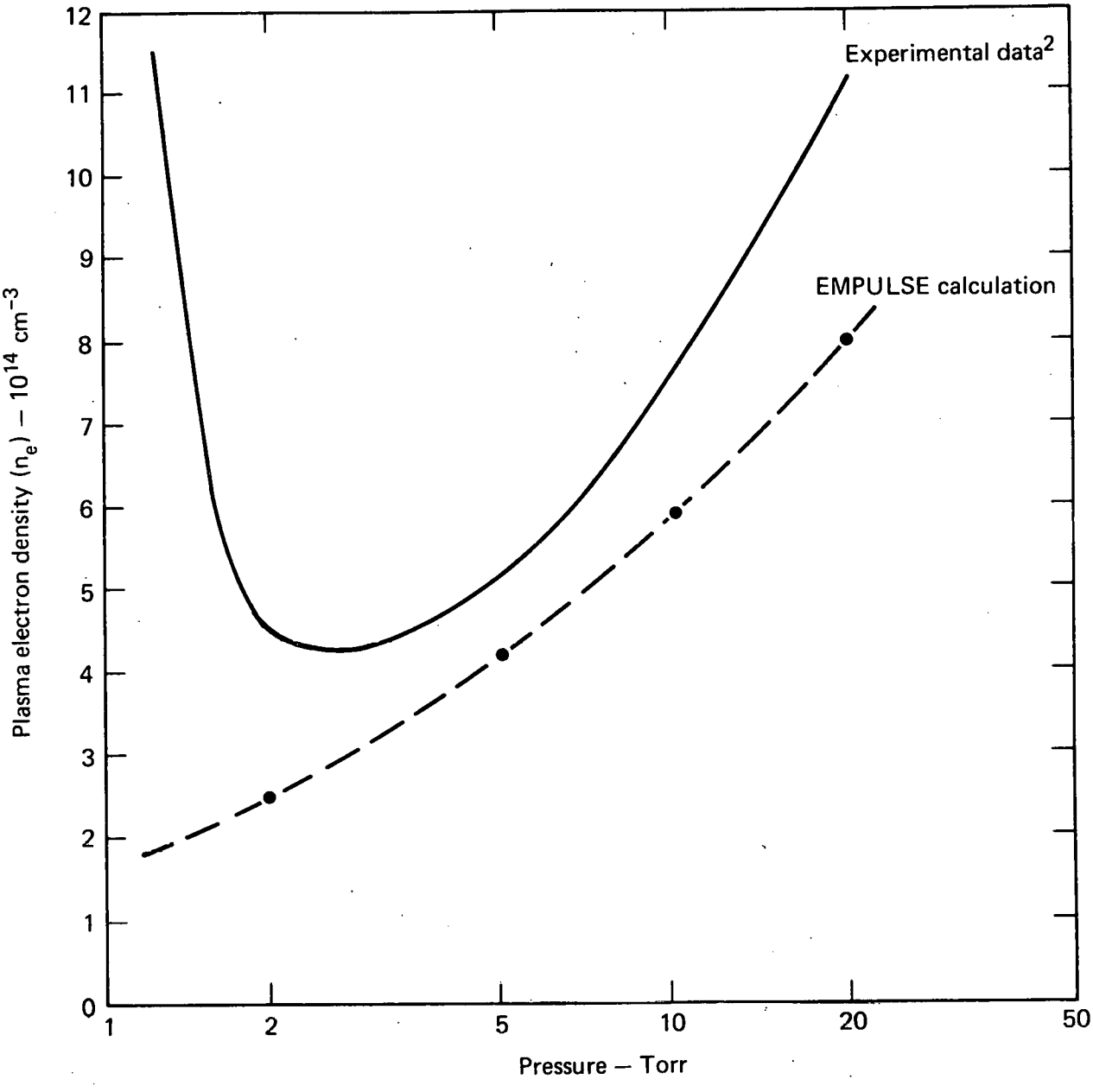

Fig. 6. Electron density as a function of pressure from both experimental data (from Ref. 2) and present EMPULSE calculations.

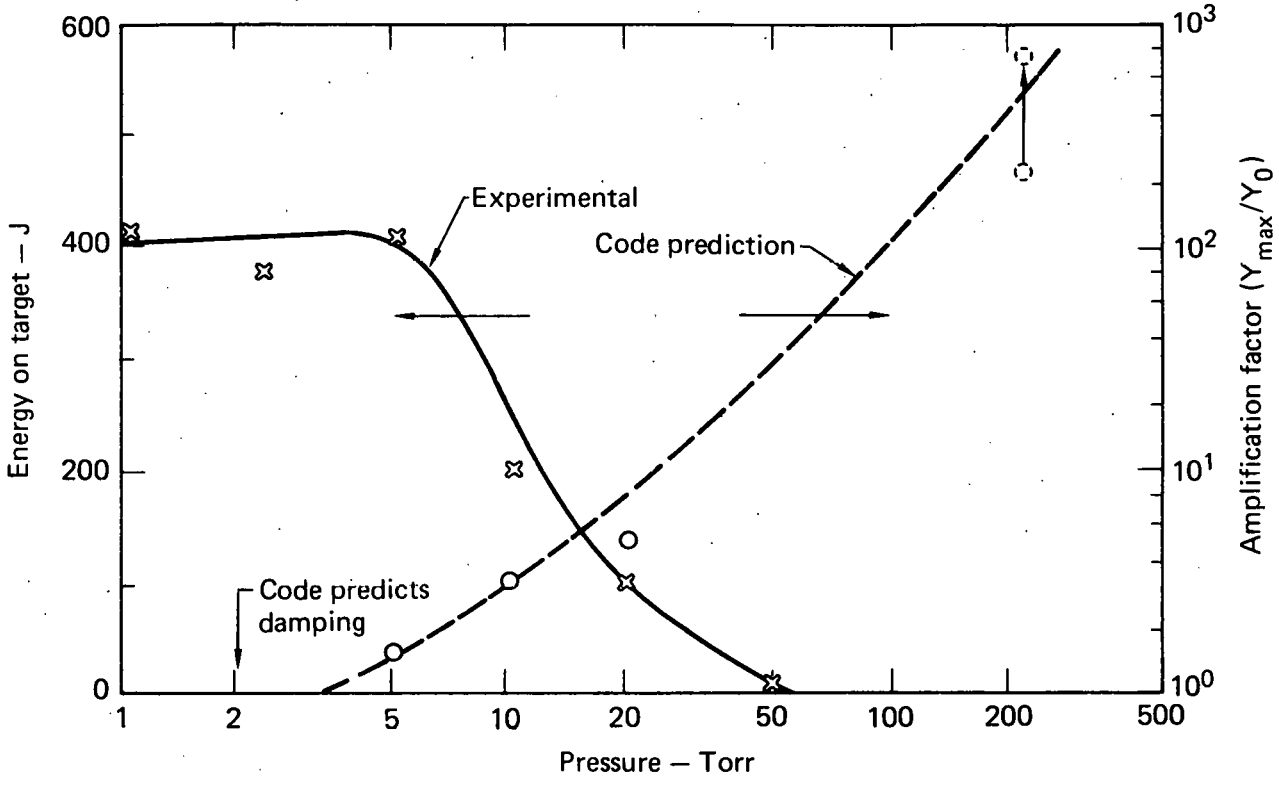

Fig. 7. Experimentally determined beam pulse energy on target at 100 cm and EMPULSE code prediction of amplification factor vs pressure.

(4) The product $n_e a^2$ is nearly independent of P for the low pressure runs; the breakdown process appears to remove a constant amount of energy from the pulse. Hence, σ and λ vary as P^{-1}, since $\nu^m \propto P$.

(5) In the pulse body, the maximum hose growth from point x_0 to x is predicted by simple analytic models to be[3]

$$Y \propto \left(\frac{x}{x_0}\right)^{\frac{0.69}{d\lambda/dx}} .$$

Valves of Y derived from this formula, using the mean value of $d\lambda/dx$, are given in Table 3. We take x_0 to be the point at which growth is first observed, and we take x = 600 cm, the point where Y_{max} is computed. Approximate agreement between EMPULSE runs and this formula is evident.

(6) In no run except P = 200 Torr is the pulse head unstable. This is a new feature in the hose stability picture predicted by EMPULSE but not yet fully understood. It is known that hose growth should be strongly suppressed at very low conductivity ($\sigma a/c < 1$), which prevails up to the pinch point. It is possible that the rapid decrease of the effective betatron period following the pinch point causes a "detuning" of the instability, with a resultant suppression of growth.

(7) Hose growth is delayed by rapid growth of σ; note that the position at which hose amplification begins (x_0) increases as P is reduced. This fact is probably explained by the competition between phase mixing and unstable growth. The damping always prevails at small x, so as hose growth is reduced, the damped zone is expanded.

(8) Finally, it is important to note that the run at P = 2 Torr shows no hose growth at all. EMPULSE can be run at yet lower pressures, but as we

Table 3. Comparison of the analytic estimate of hose growth with the growth computed with EMPULSE.

Pressure, Torr	2	5	10	20	200
Analytic estimate	-	1.4	4.3	7.2	6×10^6
EMPULSE	-	1.7	3.5	4.5	200+

have already mentioned, the results are not in accord with the experiment. A preliminary study (runs at $z = 0$ only) shows that the trend of increasing λ with decreasing P continues at least to 0.1 Torr. No "starvation" of the secondary ionization is observed in the computer runs, so the poor propagation observed in the experiments below 1 Torr do not appear to be related to hose instability. Rather, propagation in this regime can be explained by the two-stream instability, as will be discussed in a separate report.

ACKNOWLEDGMENT

This work was jointly supported by the Department of the Navy, under contract No. NAONR 11-76.

REFERENCES

1. T. J. Fessenden and J. C. Clark, *Experimental Observations of the Propagation of a 15 Kamp, 1.2 MeV, 30 ns Electron Beam,* Lawrence Livermore Livermore Laboratory, Livermore, Calif., UCID-16868 (1975).
2. J. C. Clark, T. J. Clark, T. J. Fessenden, and D. O. Trimble, *Further Experimental Observations of the Propagation of a High Current Electron Beam in Various Gases,* Lawrence Livermore Laboratory, Livermore, Calif., UCIR-979 (1976).
3. R. J. Briggs, E. P. Lee, L. D. Pearlstein, and J. M. Leary, *Stability of a High Current, Relativistic Electron Pulse,* Lawrence Livermore Laboratory, Livermore, Calif., UCID-17072 (1976) (title U, report SNSI).
4. E. P. Lee, *The New Field Equations,* Lawrence Livermore Laboratory, Livermore, Calif., UCID-17286 (1976).
5. P. Felsenthal and J. M. Proud, *Physical Review,* 139(6A) 1796 (1965).
6. E. P. Lee, "Resistive Hose Instability of a Beam with the Bennett Profile," Lawrence Livermore Laboratory, Livermore Calif., (in preparation, June 1977; to be submitted to *Physics of Fluids*).

APA/cld/vt/mla

Printed in the United States of America
Available from
National Technical Information Service
U.S. Department of Commerce
5285 Port Royal Road
Springfield, VA 22161
Price: Printed Copy $; Microfiche $3.00

Page Range	Domestic Price	Page Range	Domestic Price
001–025	$ 3.50	326–350	10.00
026–050	4.00	351–375	10.50
051–075	4.50	376–400	10.75
076–100	5.00	401–425	11.00
101–125	5.50	426–450	11.75
126–150	6.00	451–475	12.00
151–175	6.75	476–500	12.50
176–200	7.50	501–525	12.75
201–225	7.75	526–550	13.00
226–250	8.00	551–575	13.50
251–275	9.00	576–600	13.75
276–300	9.25	601–up	*
301–325	9.75		

*Add $2.50 for each additional 100 page increment from 601 to 1,000 pages; add $4.50 for each additional 100 page increment over 1,000 pages.